J Neuropathol Exp Neurol
Vol. 75, No. 9, September 2016, pp. 868–876
doi: 10.1093/jnen/nlw062

OXFORD

ORIGINAL ARTICLE

Tenascin-C Is Associated with Cored Amyloid-β Plaques in Alzheimer Disease and Pathology Burdened Cognitively Normal Elderly

Zhiping Mi, MD, Willi Halfter, PhD, Eric E. Abrahamson, PhD, William E. Klunk, MD, PhD, Chester A. Mathis, PhD, Elliott J. Mufson, PhD, and Milos D. Ikonomovic, MD

Abstract

Tenascin-C (TN-C) is an extracellular matrix glycoprotein linked to inflammatory processes in pathological conditions including Alzheimer disease (AD). We examined the distribution of TN-C immunoreactivity (ir) in relation to amyloid-β (Aβ) plaques and vascular Aβ deposits in autopsy brain tissues from 14 patients with clinical and neuropathological AD and 10 aged-matched controls with no cognitive impairment; 5 of the controls had Aβ plaques and 5 did not. TN-C ir was abundant in cortical white matter and subpial cerebral gray matter in all cases, whereas TN-C ir was weak in blood vessels. In all cases with Aβ plaques but not in plaque-free controls, TN-C ir was detected as large (>100 μm in diameter) diffuse extracellular deposits in cortical grey matter. TN-C plaques completely overlapped and surrounded cored Aβ plaques labeled with X-34, a fluorescent derivative of Congo red, and they were associated with reactive astrocytes astrocytes, microglia and phosphorylated tau-containing dystrophic neurites. Diffuse Aβ plaques lacking amyloid cores, reactive glia or dystrophic neurites showed no TN-C ir. In cases with cerebral amyloid angiopathy, TN-C ir in vessel walls did not spread into the surrounding neuropil. These results suggest a role for TN-C in Aβ plaque pathogenesis and its potential as a biomarker and therapy target.

From the [1]Departments of Neurology (ZM, EEA, WEK, MDI), [2]Neurobiology (WH), [3]Psychiatry (WEK, MDI), [4]Radiology, University of Pittsburgh (CAM), [5]Geriatric Research Education and Clinical Center, VA Pittsburgh Healthcare System (ZM, EEA, MDI), and [6]Department of Neurobiology, Barrow Neurological Institute, Pittsburgh, PA, USA (EJM)

Send correspondence to: Milos D. Ikonomovic, MD, Department of Neurology, University of Pittsburgh School of Medicine, 200 Lothrop Street, BST south, Room S521, Pittsburgh, PA 15213, USA, E-mail: ikonomovicmd@upmc.edu

This study was supported by grants PO1AG014449, AG05133 (University of Pittsburgh ADRC), PO1AG025204, and RO1AG43775 from the National Institute on Aging, National Institutes of Health and the Barrow Neurological Institute Barrow and Beyond.

Zhiping Mi, Willi Halfter and Eric E. Abrahamson declare no conflict of interest. William E. Klunk and Chester A. Mathis are co-inventors of PiB and have financial interest in a license agreement between University of Pittsburgh and GE Healthcare based on the PiB technology. Elliott J. Mufson has served as consultant to NeuroPhage Pharmaceuticals, Inc. Milos D. Ikonomovic has served as consultant to and has received research grants from GE Healthcare.

Key Words: β-amyloid, Alzheimer disease, Astrocytes, Extracellular matrix, Inflammation, Microglia, Tau, Tenascin.

INTRODUCTION

Alzheimer disease (AD) is a chronic neurodegenerative disorder characterized histopathologically by extracellular amyloid plaques and intracellular neurofibrillary tangles. The principal component of amyloid plaques is the amyloid β (Aβ) peptide, a 39–43 amino acid fragment proteolytically produced from a transmembrane Aβ precursor protein (APP) (1–3). Numerous extracellular proteins bind to or colocalize with Aβ in AD plaques. These include inflammatory molecules (acute phase proteins, cytokines, chemokines, complement proteins) (4), amyloidogenic molecules (apolipoproteins and the non-Aβ component of AD amyloid, NAC) (5), lysosomal proteinases and ubiquitin (5) and numerous extracellular matrix (ECM) proteins including proteoglycans (heparan, chondroitin, keratin and dermatan sulphate proteoglycans) (6–10), reelin, agrin, collagen XVIII, collagen-like Alzheimer amyloid plaque component, ECM modulator lysyl oxidase, tissue inhibitor of matrix metalloproteinases and Goodpasture antigen-binding protein/ceramide transporter (11–16). The role of plaque-associated proteins in initiation or dissolution of Aβ aggregates in AD is poorly understood.

Tenascin-C (TN-C) is an ECM glycoprotein that regulates the differentiation and proliferation of astrocytes during embryogenesis and CNS development (17–19). TN-C expression is downregulated in the adult brain but it can be increased due to inflammatory processes and injuries to the nervous system (20, 21). A recent study suggested that TN-C is involved in the pathogenesis of AD: TN-C gene transcription increased in microglia after they were exposed to Aβ, and brains of transgenic mice overexpressing APP had increased TN-C expression whereas Aβ plaque burden was reduced in TN-C-deficient APP mice (22). These associations warrant detailed investigations of brains from AD patients compared with normal elderly subjects. In this study, we examined localization of TN-C immunoreactivity (ir) in relation to Aβ pathology burden as well as inflammatory markers and phosphorylated

tau in postmortem brain tissue from AD cases and age-matched cognitively normal controls.

MATERIALS AND METHODS

Protocol Approvals and Patient Consent

The study was approved by Rush University and the University of Pittsburgh's Committee for Oversight of Research and Clinical Training Involving Decedents. Written informed consent for research and autopsy was obtained for all subjects in the study.

Cases

The brains of 24 cases were evaluated (Table 1); these included 19 from the Rush Religious Order Study, a longitudinal clinical-pathologic study of aging and AD in older Catholic nuns, priests, and brothers who died with a premortem clinical diagnosis of "no cognitive impairment" ([NCI], n = 10) or "mild-moderate AD" (n = 9) and received a neuropathological evaluation postmortem (23). An additional 5 cases with moderate-severe AD were participants in the University of Pittsburgh Alzheimer's Disease Research Center. Details of clinical evaluation and diagnostic criteria were published previously (23, 24). A consensus conference of neurologists and neuropsychologists reviewed clinical data, medical records and interviews with family members and assigned a final clinical diagnosis. Mini-Mental State Examination (25) scores in the AD group ranged from 6 to 25 (Table 1). Neuropathologic diagnoses were based on the National Institute on Aging (NIA)–Reagan Institute criteria (NIA-RI Working Group) (26), recommendations of the Consortium to Establish a Registry for Alzheimer's Disease (CERAD) (27) and Braak staging of neurofibrillary tangles (28). Application of the new National Institute on Aging-Alzheimer's Association guidelines (29) is currently ongoing in the examined cohorts. Cases with strokes, Lewy body disease, Parkinson disease or hippocampal sclerosis were excluded. All cases were de-identified and randomly assigned a unique identifier prior to the study.

Tissue Preparation

At autopsy (mean postmortem interval 6.6 hours, range 2.2–11 hours; Table 1), superior frontal cortex (Brodmann area 9), caudate nucleus, and cerebellum were dissected and immersed in 4% paraformaldehyde in sodium phosphate buffer ([PB], pH 7.4), for 48 hours, cryoprotected in glycol solution (30), and sectioned at 40 μm on a freezing sliding microtome. Sections were then stored in cryoprotection solution (31) at –20 °C until processing.

Immunohistochemistry and Histology

Chemicals were purchased from Sigma-Aldrich (St. Louis, MO) unless otherwise indicated. Table 2 lists all histological compounds and antibodies used in the study.

TN-C Immunofluorescence. Tissue sections were washed in PB, incubated for 1 hour in PB containing 0.3% Triton X-100, 3% normal goat serum and 2% bovine serum albumin, followed by an overnight incubation at 4 °C in monoclonal antibody (mab) B28-13 (diluted 1:500, provided by Dr. Ruth Chiquet-Ehrismann, University of Basel, Basel, Switzerland) raised against human TN-C, with its binding site localized to the last 3 fibronectin type III repeats, and its specificity confirmed previously by Western blotting and immunocytochemistry (32). Tissue sections were subsequently incubated for 2 hours with affinity purified goat anti-mouse IgG (Cy3; 1:500 dilution; Jackson ImmunoResearch Laboratories, West Grove, PA). Control sections processed in the absence of TN-C antibody resulted in no immunoreactivity.

Combined Immunofluorescence and Histofluorescence. To assess co-distribution of ECM proteins with fibrillar Aβ deposits, tissue sections were first processed as described above using antibodies generated against TN-C (mab B28-13; diluted 1:500), collagen IV (600-401-106-0.5; rabbit polyclonal; diluted 1: 1000; Rockland, Gilbertsville, PA), fibronectin (mab 1940; diluted 1: 500; EMD Millipore, Billerica, MA), or agrin (rabbit polyclonal; 1:50; gift from Dr. Gregory Cole, North Carolina Central University, Durham, NC) (12), followed by an affinity purified species-appropriate secondary IgG (Cy2 and Cy3; 1:500 dilution; Jackson ImmunoResearch Laboratories). Sections were then processed for X-34 (100 μM, a highly fluorescent derivative of Congo red) or 6-CN-Pittsburgh Compound B (6-CN-PiB) (10 μM, a highly fluorescent derivative of PiB), as previously described in (33).

Multiple-Labeling Immunofluorescence. Sections were rinsed in PB, treated with 85% formic acid for 2 min, and incubated in a cocktail of TN-C antibody (mab B28-13; diluted 1:500) and rabbit polyclonal antibodies against Aβ40 (AB5078P; 1:200; Millipore) and Aβ42 (AB5074P; 1:200; Millipore) overnight at 4 °C. Sections were then incubated in a cocktail of affinity purified goat anti-mouse IgG (Cy3; 1:500 dilution; Jackson ImmunoResearch Laboratories) and goat-anti-rabbit IgG (Alexa488; 1:500 dilution; ThermoFisher Scientific, Grand Island, NY) secondary antibodies for 3 hours at room temperature. To assess co-distribution of TN-C with phosphorylated tau, astrocytes, and microglia, sections were processed as described above (with the omission of formic acid pretreatment) using a cocktail of TN-C antibody (mab B28-13; diluted 1:500) and polyclonal antibodies against either tau phosphorylated at Serine 404 (ab30666, diluted 1:500; Abcam, Cambridge, MA), glial fibrillary acidic protein ([GFAP], ab4674; diluted 1:500; Abcam), or ionized calcium binding adaptor molecule 1 ([Iba1], 091-19741; diluted 1:500; Wako, Richmond, VA). Sections were then processed in a cocktail of species-appropriate secondary antibodies: goat anti-mouse IgG (Cy3; 1:500 dilution; Jackson ImmunoResearch Laboratories) for TN-C; goat-anti-rabbit IgG (Alexa488; 1:500 dilution; ThermoFisher Scientific) for phosphorylated tau and Iba1; goat-anti-chicken (Alexa488; 1:500 dilution; ThermoFisher Scientific) for GFAP.

Quantitative Analyses of TN-C and Aβ-Immunoreactive Plaques in the Frontal Cortex

Analyses of TN-C and Aβ Plaque Count. Numbers of total and co-labeled TN-C and Aβ40/42-immunoreactive (-ir) plaques were counted in three randomly selected, non-overlapping 10× microscopic fields (2.35 mm^2 field of

TABLE 1. Demographic, Clinical and Neuropathological Characteristics by Clinical Diagnosis Category

	Clinical diagnosis			
	NCI (n = 10)	AD (n = 14)	Total (n = 24)	p value
Age (years) at death:				
Mean ± SD (Range)	84.3 ± 5.3 (74.0–93.0)	85.1 ± 6.6 (69.0–94.0)	84.8 ± 5.9 (69.0–94.0)	0.60[m]
Number (%) of males:	6 (50.0%)	6 (50.0%)	12 (50.0%)	0.68[f]
MMSE: Mean ± SD (Range)	27.0 ± 1.5 (25-30)	16.9 ± 7.8 (6-25)	21.1 ± 7.8 (6-30)	0.0001[m]
PMI (h):				
Mean ± SD (Range)	6.7 ± 3.2 (2.2–11.0)	6.6 ± 2.8 (3.0–10.7)	6.6 ± 2.9 (2.2–11.0)	0.80[m]
Braak scores:				
0	2	0	2	
I/II	2	0	2	0.0001[m]
III/IV	6	4	10	
V/VI	0	10	10	
CERAD diagnosis:				
No AD	5	0	5	
Possible	5	0	5	
Probable	0	5	5	0.001[m]
Definite	0	9	9	
NIA-RI diagnosis				
No AD	2	0	2	
Low	4	0	4	
Intermediate	4	6	10	0.0001[m]
High	0	8	8	

NCI, no cognitive impairment; AD, Alzheimer disease; PMI, postmortem interval; MMSE, Mini-Mental State Examination; CERAD, Consortium to Establish a Registry for Alzheimer's Disease; NIA-RI, National Institute on Aging-Reagan Institute; [f]Fisher's exact test; [m]Mann-Whitney U test.

TABLE 2. Histological Compounds and Antibodies

Compound	Affinity	Concentration	Source
X-34	β-Pleated sheet	100 μM	Synthesized (69)
6-CN-PiB	Amyloid-beta fibrils	10 μM	Synthesized (33)
Antibody (host)	**Epitope or immunogen**	**Dilution**	**Source**
TN-C (mouse)	Human TN-C	1:500	Generated by R. Chiquet-Ehrismann (32)
Aβx-42 (rabbit)	Aβx-42	1:200	Millipore
Aβx-40 (rabbit)	Aβx-40	1:200	Millipore
Iba1(rabbit)	A synthetic peptide corresponding to C-terminus of Iba1	1:500	Wako
GFAP (chick)	Bovine GFAP	1:1000	Abcam
Fibronectin (mouse)	Extra domain A	1:500	Millipore
Agrin (rabbit)	Human agrin	1:50	Generated by G. J. Cole (12)
Collagen IV (rabbit)	Human and bovine placenta	1:1000	Rockland
Phosphorylated tau (rabbit)	Serine 404	1:1000	Abcam

view), in 3 sections per case. Results are expressed as mean ± SD.

Analyses of TN-C and Aβ Plaque Loads (Percent Area). Percent areal coverages for TN-C and Aβ40/42-ir plaques were determined in the same 10× microscopic fields used for plaque count analyses. Percent area values were obtained by dividing immunolabeled area by total area sampled. Fluorescence illumination intensity was held constant throughout the sampling procedure and images were analyzed using the public domain ImageJ program (available at: http://rsb.info.nih.gov/nihimage/). A predetermined threshold value was held constant throughout the analysis.

Statistical Analysis

Statistical comparisons of the demographic, cognitive, and neuropathologic data between AD and NCI groups were performed using the Fisher exact test (gender) and Mann Whitney *U* test (age, postmortem interval, MMSE, NIA-RI diagnoses of AD, CERAD and Braak scores). TN-C and

Aβ40/42 plaque counts and load were compared in AD and NCI cases using the Student *t*-test. Correlation analyses were performed using Spearman correlation. Statistical significance was set at 0.05 (two-sided).

RESULTS

Table 1 shows demographic, cognitive, and neuropathologic characteristics of the subjects grouped by clinical diagnosis. The NCI and AD groups did not differ significantly by age, gender, or postmortem interval. However, the 2 groups differed significantly by MMSE, Braak scores, CERAD and NIA-RI diagnosis of AD, although the NCI group included Aβ plaque pathology burdened (Aβ-positive NCI, $n = 5$) and Aβ pathology-free (Aβ-negative NCI, $n = 5$) cases.

In the frontal cortex from all AD and NCI cases, intense homogeneous TN-C ir was observed in the white matter (WM) and subpial portion of gray matter (Fig. 1A, B), whereas weaker TN-C ir was seen in cortical blood vessels (Fig. 1C). In AD and Aβ-positive NCI, TN-C-ir plaques were observed in the cortical gray matter; they ranged in diameter from 80 to 200 μm (average 120 ± 20 μm) and were more frequent in deep cortical layers, consistent with known distribution of classic neuritic plaques in the frontal cortex (34). TN-C plaques were not detected in Aβ-negative NCI cases. Quantitative analyses showed that compared with the Aβ-positive NCI, AD cases had significantly higher numbers of TN-C and Aβ plaques in the frontal cortex (TN-C count: $p = 0.004$, Aβ plaque count: $p = 0.0001$) and higher plaque loads by percent area (TN-C percent area: $p = 0.001$; Aβ percent area: $p = 0.029$). TN-C plaques completely surrounded cored Aβ plaques (Fig. 1C–F), which co-labeled with X-34, a highly fluorescent derivative of Congo red (Fig. 2A). There was a significant correlation ($R^2 = 0.98$; $p < 0.001$) between numbers of TN-C plaques and cored Aβ plaques. The majority of TN-C plaques (73%) surrounded cored Aβ plaques, whereas approximately 80% of cored Aβ plaques were observed inside TN-C plaques.

Immunoreactivity for 2 other ECM proteins, collagen IV (Fig. 2B) and fibronectin (not shown), was restricted to blood vessels and did not colocalize with X-34 and Aβ-ir plaques. The ECM protein agrin ir localized to both blood vessels and cored Aβ plaques, but in contrast to TN-C it did not extend beyond the plaque halos (Fig. 2C–E). No ECM protein ir was found in diffuse (non-cored) Aβ plaques (not shown).

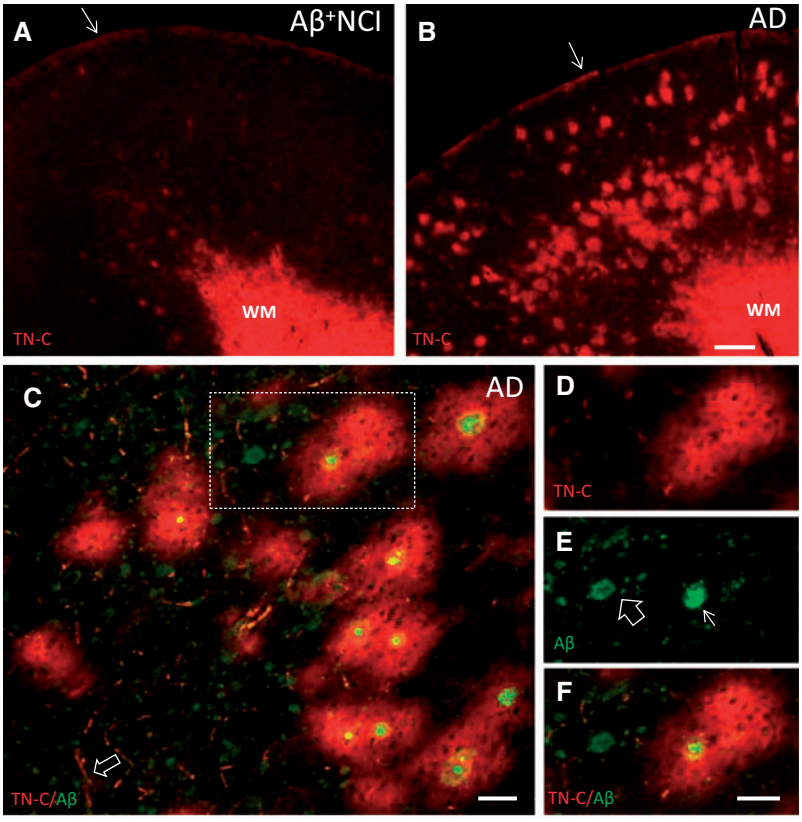

FIGURE 1. TN-C immunofluorescence in the frontal cortex from representative Aβ plaque burdened NCI **(A)** and AD **(B)** cases. Dense TN-C ir is present in the WM and subpial layer (arrows) in both cases, whereas TN-C deposits in the gray matter are more abundant in AD. **(C)** Section of frontal cortex from an AD case processed for dual immunofluorescence with antibodies against TN-C (red) and Aβ (green) showing that the majority of large TN-C deposits completely surround cored Aβ plaques. TN-C-labeled blood vessels are also seen (arrow). **(D-F)** TN-C/Aβ dual-immunolabeling in the area boxed in **C**. TN-C ir (D, red) surrounds the cored Aβ plaque (arrow in **E**, green) while the diffuse Aβ plaque (open arrow in **E**, green) is not associated with TN-C ir. Merged image is shown in **(F)**. Scale bars: bar in **A** = 500 μm (for **A** and **B**); bar in **C** =50 μm; bar in **D** = 50 μm (for **D-F**).

Overlap of TN-C plaques with diffuse Aβ plaques was observed only when cored and diffuse Aβ plaques were in close proximity.

Cored Aβ plaques surrounded by TN-C plaques were also strongly labeled with 6-CN-PiB, a highly fluorescent derivative of the amyloid-binding compound PiB, and contained reactive glia, with GFAP-ir astrocytes restricted to the periphery (Fig. 3A–D), whereas Iba1-ir microglia clustered at the Aβ plaque core (Fig. 3E–H). TN-C/6-CN-PiB co-labeled plaques also contained phosphorylated-tau-ir dystrophic neurites (Fig. 4).

As in the frontal cortex, TN-C ir was robust in the WM of the cerebellum and caudate nucleus where it labeled large bundles of myelinated fibers, while TN-C ir was not observed in diffuse Aβ plaques in these brain regions. Cerebral vascular localization of TN-C ir was less prominent in Aβ-burdened blood vessels (cerebral amyloid angiopathy [CAA]) observed in a subset of AD cases (not shown). In contrast to the association with cored plaques, TN-C did not form a halo or patch around CAA, but when cored Aβ plaques were positioned in close proximity to blood vessels TN-C ir was also seen around the blood vessels, regardless of whether the vessels were affected with CAA or not (not shown).

DISCUSSION

This report provides novel information regarding the localization of TN-C in the brains of AD and elderly people with NCI. We observed large TN-C-ir diffuse extracellular deposits in the frontal cortex of AD and Aβ pathology-burdened NCI, which is considered preclinical AD (35, 36), while such deposits were absent from the NCI brains that were free of Aβ plaques. TN-C deposits colocalized with and surrounded cored neuritic Aβ plaques, but they did not associate with diffuse Aβ plaques lacking X-34 and a 6-CN-PiB-positive core, reactive astrocytes and microglia, and phosphorylated tau-containing dystrophic neurites. These results suggest a role for TN-C in the development of, or reaction to, classic senile plaques in AD. We also observed TN-C ir cerebral blood vessels in all cases regardless of clinical and pathology status; this is in agreement with previous reports of TN-C ir vasculature in brain (37) and other tissues (38). However, we found that when associated with CAA, which consists of fibrillar Aβ deposits similar to those in amyloid plaques, TN-C ir was weak and rarely extended into surrounding parenchyma. This might be due to lesser microgliosis associated with CAA-burdened vessels compared with cored plaques (39, 40) and decreased ECM proteins; the latter may possibly relate to their susceptibility to rupture (41). Thus, reduced TN-C content in CAA relative to normal blood vessels might contribute to the progression of vascular pathology in AD.

The source of TN-C surrounding cored Aβ plaques and the temporal sequence of its accumulation in relation to aggregated Aβ and phosphorylated tau are not clear. We observed robust TN-C ir in the cortical WM and layer I in all AD and NCI cases. This is in agreement with reports of greater TN-C expression in the WM compared with gray matter in normal human brain (42), and of TN-C synthesis by astrocytes and release into the extracellular environment of WM and layer I of the cortex (42, 43). We also found that TN-C plaques surrounding cored Aβ plaques were permeated by reactive astrocytes and their processes whereas microglia were in closer contact with cored Aβ plaques. This distribution pattern of activated glia has been described in classic neuritic plaques of AD and in old APPV717F mice (44, 45). Inflammatory cells, specifically interleukin-1 (IL-1)-expressing microglia and S100β-producing astrocytes, are believed to play major roles in the formation of neuritic plaques with tau-positive dystrophic neurites (4, 46, 47). In addition to activating the astrocytes, IL-1 upregulates APP and thereby stimulates Aβ production. Microglia can also stimulate astrocyte proliferation via TGF-β1 (48, 49), and increased GFAP production (50) induces TN-C gene expression and TN-C protein production (51–53). Furthermore, TN-C is an endogenous activator of Toll-like receptor, which induces the expression of proinflammatory factors (54). Overall, these observations support a role for TN-C in brain inflammation (42, 55–57), which is closely linked to Aβ deposition in AD. In mice overexpressing mutant human APP, higher levels of TN-C gene transcription were associated with more advanced Aβ plaque pathology and inflammatory reaction, while TN-C deficiency reduced proinflammatory activation and fibrillar Aβ concentration (22). Other studies provide additional evidence that TN-C influences the development or progression of neuritic Aβ plaques. TN-C stimulates the expression of 14-3-3 (a family of homologous proteins that consist of seven isoforms [β, γ, ϵ, η, ζ, σ, and τ/θ]) (58, 59), which can bind tau (60, 61) and regulate tau phosphorylation via glycogen synthase kinase-3 beta (GSK3β) (61, 62). Furthermore, 14-3-3ζ can bridge the interaction of GSK3ζ with tau and facilitate GSK3β-mediated phosphorylation of tau (63). Additional studies using in vitro and appropriate transgenic AD models are needed to elucidate these pathological pathways.

Because TN-C deposits surrounded selectively cored neuritic Aβ plaques, our results also suggest a potential value for TN-C as an AD biomarker that may have diagnostic value in neuropathological evaluation of AD (27, 64). Neuritic plaques are considered to be the prime target for amyloid PET imaging (65–68). While current PET radioligands cannot distinguish between cored/neuritic and diffuse plaques (69, 70), or between parenchymal plaques and CAA (69, 71), a TN-C PET tracer might show selectivity for cored Aβ plaques in the gray matter. However, the marked TN-C staining seen in the WM would present a considerable obstacle in PET imaging studies of brain amyloidosis. On the other hand, the use of TN-C as a CSF or blood biomarker for AD-associated brain amyloidosis and inflammation should be considered (72).

Some methodological considerations warrant further discussion. The observed 73% overlap of TN-C deposits with cored Aβ plaques is likely an underestimation because TN-C deposits are substantially larger and completely surround cored Aβ plaques, Thus, in some instances TN-C plaques with only the peripheral halo but not the core of Aβ plaques (or no Aβ plaque at all) can be present in the plane of section. It is also possible that our immunostaining assay is not sensitive enough to detect the TN-C around all cored Aβ plaques. A systematic evaluation of TN-C negative cored Aβ plaques in relation to markers of microglia and astrocytes as well as

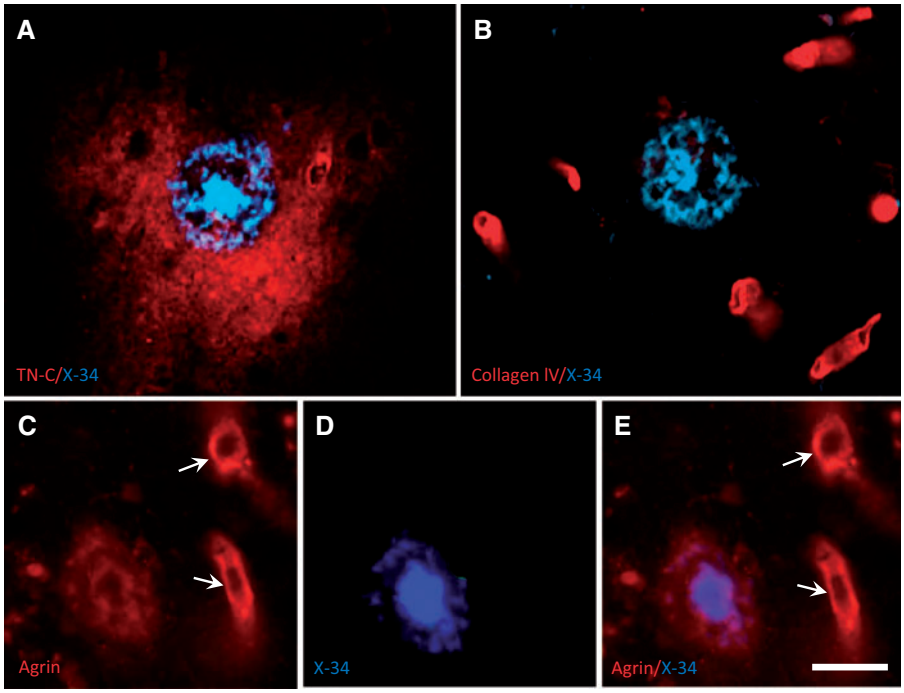

FIGURE 2. High-magnification fluorescence microscopy images of frontal cortex tissue sections from an AD case, processed for dual labeling with X-34 and extracellular matrix proteins. **(A)** Typical X-34-labeled cored amyloid plaque (blue) is completely surrounded by larger diffuse TN-C deposit (red). **(B)** Collagen IV is detected exclusively in blood vessels (red) and is not seen in the X-34-labeled cored plaque (blue). **(C–E)** A proteoglycan agrin (red) is present in blood vessels (arrows) and in the periphery, but not the central core, of an X-34-positive Aβ plaque (blue). Scale bar: **A**–**E** = 30 μm.

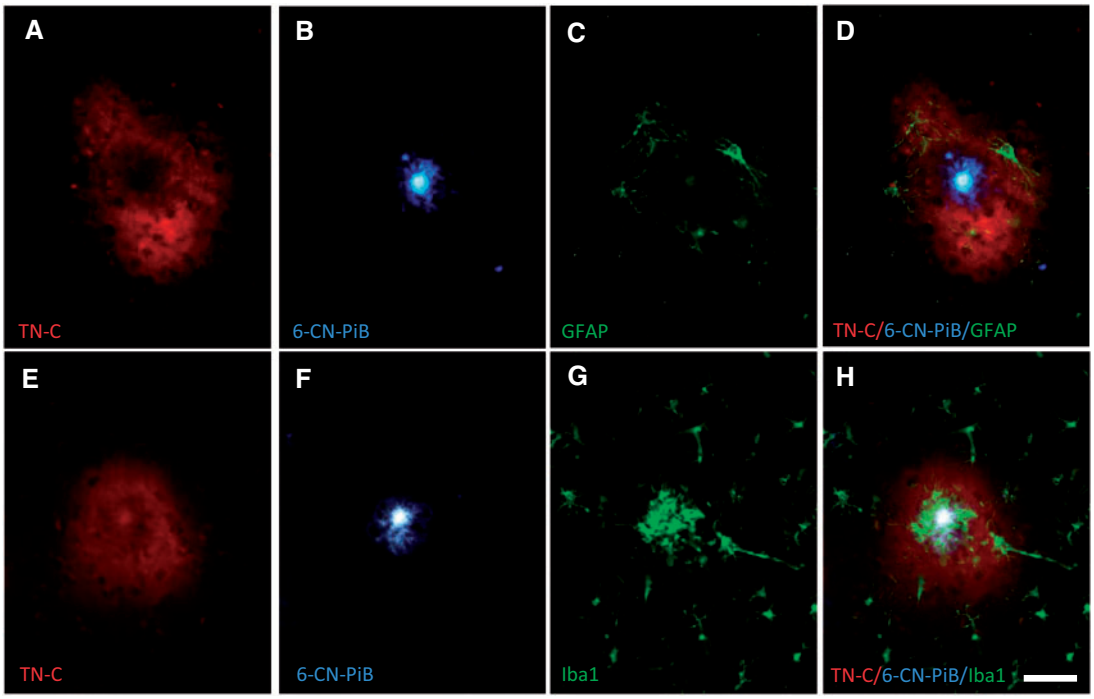

FIGURE 3. Triple fluorescent labeling in a single section of frontal cortex from an AD case. TN-C-ir deposits (**A** and **E**, red) completely surround 6-CN-PiB-labeled cored amyloid plaques (**B** and **F**, blue) with GFAP-ir astrocytes located near the periphery (**C**, green) and Iba1-ir microglia at the center (**G**, green) of the plaque. Panels **D** and **H** are merged fluorescence images of **A**–**C** and **E**–**G**, respectively. Scale bar: **A**–**H** = 50 μm.

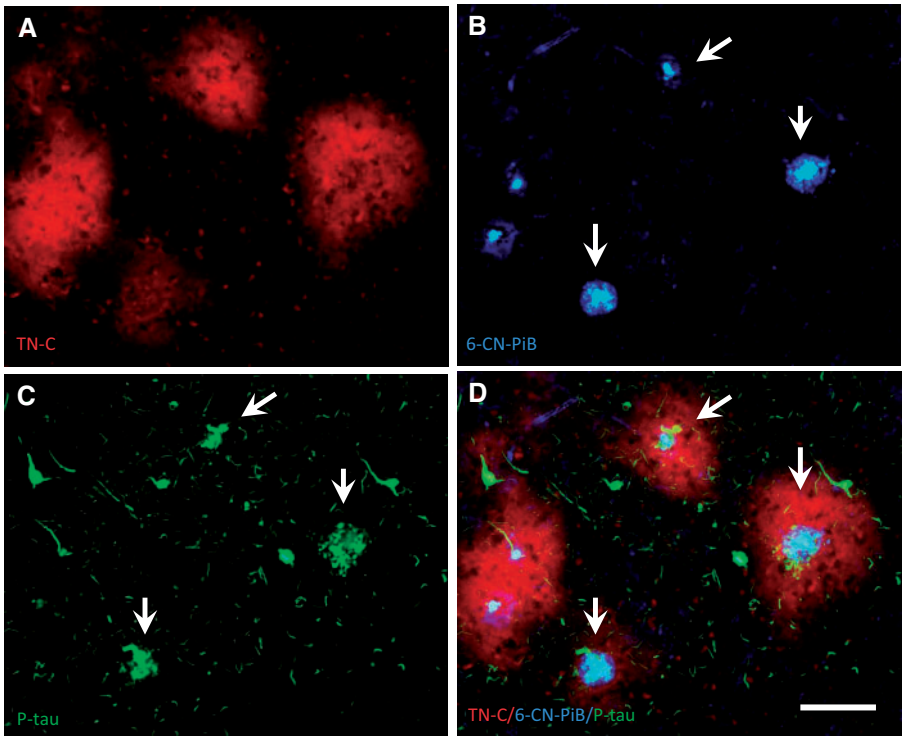

FIGURE 4. Triple fluorescent labeling in a single section of frontal cortex from an AD case. Large TN-C deposits (**A**, red) contain 6-CN-PiB-positive cored plaques (**B**, blue) surrounded by clusters of phosphorylated-tau-ir dystrophic neurites (**C**, green, arrows), whereas individual phosphorylated-tau-ir tangles show no TN-C immunofluorescence. Panel **D** shows merged fluorescence, with typical cored neuritic Aβ plaques surrounded by TN-C plaques (arrows in **B**–**D**). Scale bar: **A**–**D** = 100 μm.

related inflammatory molecules will provide greater insight into this issue.

In summary, in AD and Aβ plaque-burdened cognitively normal elderly subjects, cortical TN-C deposits colocalized with and selectively surrounded cored Aβ plaques that labeled with PiB and X-34. The deposits were closely associated with inflammatory cells and phosphorylated tau containing dystrophic neurites. Collectively, our data suggest that TN-C plays a role in reactive processes involved either in the progression or clearance of amyloid plaques. These complex relationships could not be determined in the current cross-sectional analysis, thus the potential value of TN-C as a biomarker and target for therapy in AD remains to be investigated.

ACKNOWLEDGMENTS

The authors wish to thank Dr. Ruth Chiquet-Ehrismann for providing the TN-C antibody, Dr. Michael H. Ahmadi for statistical assistance, and Angela Ye Weon Ryu, Lan Shao and William Paljug for technical assistance. We are grateful to the participants in the Rush Religious Orders Study and University of Pittsburgh ADRC.

REFERENCES

1. Masters CL, Simms G, Weinman NA, et al. Amyloid plaque core protein in Alzheimer disease and Down syndrome. Proc Natl Acad Sci U S A 1985;82:4245–9
2. Kang J, Lemaire HG, Unterbeck A, et al. The precursor of Alzheimer's disease amyloid A4 protein resembles a cell-surface receptor. Nature 1987;325:733–6
3. Esler WP, Wolfe MS. A portrait of Alzheimer secretases–new features and familiar faces. Science 2001;293:1449–54
4. Griffin WS, Sheng JG, Roberts GW, et al. Interleukin-1 expression in different plaque types in Alzheimer's disease: significance in plaque evolution. J Neuropathol Exp Neurol 1995;54:276–81
5. Atwood CS, Martins RN, Smith MA, et al. Senile plaque composition and posttranslational modification of amyloid-beta peptide and associated proteins. Peptides 2002:23;1343–50
6. McLaurin J, Yang D, Yip CM, et al. Review: modulating factors in amyloid-beta fibril formation. J Struct Biol 2000;130:259–70
7. Snow AD, Mar H, Nochlin D, et al. The presence of heparan sulfate proteoglycans in the neuritic plaques and congophilic angiopathy in Alzheimer's disease. Am J Pathol 1988;133:456–63
8. DeWitt DA, Silver J, Canning DR, et al. Chondroitin sulfate proteoglycans are associated with the lesions of Alzheimer's disease. Exp Neurol 1993;121:149–52
9. Snow AD, Nochlin D, Sekiguichi R, et al. Identification in immunolocalization of a new class of proteoglycan (keratan sulfate) to the neuritic plaques of Alzheimer's disease. Exp Neurol 1996;138:305–17
10. Snow AD, Mar H, Nochlin D, et al. Peripheral distribution of dermatan sulfate proteoglycans (decorin) in amyloid-containing plaques and their presence in neurofibrillary tangles of Alzheimer's disease. J Histochem Cytochem 1992:40;105–13
11. Doehner J, Madhusudan A, Konietzko U, et al. Co-localization of Reelin and proteolytic AbetaPP fragments in hippocampal plaques in aged wild-type mice. J Alzheimers Dis 2010;19:1339–57
12. Cotman SL, Halfter W, Cole GJ. Agrin binds to beta-amyloid (Abeta), accelerates abeta fibril formation, and is localized to Abeta deposits in Alzheimer's disease brain. Mol Cell Neurosci 2000;15:183–98

13. van Horssen J, Wilhelmus MM, Heljasvaara R, et al. Collagen XVIII: a novel heparan sulfate proteoglycan associated with vascular amyloid depositions and senile plaques in Alzheimer's disease brains. Brain Pathol 2002:12;456–62
14. Hashimoto T, Wakabayashi T, Watanabe A, et al. CLAC: a novel Alzheimer amyloid plaque component derived from a transmembrane precursor, CLAC-P/collagen type XXV. Embo J 2002;21:1524–34
15. Peress N, Perillo E, Zucker S. Localization of tissue inhibitor of matrix metalloproteinases in Alzheimer's disease and normal brain. J Neuropathol Exp Neurol 1995;54:16–22
16. Mencarelli C, Bode GH, Losen M, et al. Goodpasture antigen-binding protein/ceramide transporter binds to human serum amyloid P-component and is present in brain amyloid plaques. J Biol Chem 2012;287: 14897–911
17. Chiquet-Ehrismann R, Tucker RP. Tenascins and the importance of adhesion modulation. Cold Spring Harb Perspect Biol 2011;3:a004960
18. Jones EV, Bouvier DS. Astrocyte-secreted matricellular proteins in CNS remodelling during development and disease. Neural Plast 2014;2014: 321209:1–12
19. Smith GM, Hale JH. Macrophage/Microglia regulation of astrocytic tenascin: synergistic action of transforming growth factor-beta and basic fibroblast growth factor. J Neurosci 1997;17:9624–33
20. Laywell ED, Dorries U, Bartsch U, et al. Enhanced expression of the developmentally regulated extracellular matrix molecule tenascin following adult brain injury. Proc Natl Acad Sci U S A 1992;89:2634–8
21. Roll L, Faissner A. Influence of the extracellular matrix on endogenous and transplanted stem cells after brain damage. Front Cell Neurosci 2014;8:219
22. Xie K, Liu Y, Hao W, et al. Tenascin-C deficiency ameliorates Alzheimer's disease-related pathology in mice. Neurobiol Aging 2013;34: 2389–98
23. Bennett DA, Wilson RS, Schneider JA, et al. Natural history of mild cognitive impairment in older persons. Neurology 2002;59:198–205
24. McKhann G, Drachman D, Folstein M, et al. Clinical diagnosis of Alzheimer's disease: report of the NINCDS-ADRDA Work Group under the auspices of Department of Health and Human Services Task Force on Alzheimer's Disease. Neurology 1984;34:939–44
25. Folstein MF, Folstein SE, McHugh PR. "Mini-mental state". A practical method for grading the cognitive state of Patients for the clinician. J Psychiatr Res 1975;12:189–98
26. Consensus report of the Working Group on: "Molecular and Biochemical Markers of Alzheimer's Disease". The Ronald and Nancy Reagan Research Institute of the Alzheimer's Association and the National Institute on Aging Working Group. Neurobiol Aging 1998;19:109–16.
27. Mirra SS, Heyman A, McKeel D, et al. The Consortium to Establish a Registry for Alzheimer's Disease (CERAD). Part II. Standardization of the neuropathologic assessment of Alzheimer's disease. Neurology 1991;41:479–86
28. Braak H, Braak E. Neuropathological stageing of Alzheimer-related changes. Acta Neuropathol 1991;82:239–59
29. Hyman BT, Phelps CH, Beach TG, et al. National Institute on Aging-Alzheimer's Association guidelines for the neuropathologic assessment of Alzheimer's disease. Alzheimers Dement 2012;8:1–13
30. Ikonomovic MD, Abrahamson EE, Isanski BA, et al. Superior frontal cortex cholinergic axon density in mild cognitive impairment and early Alzheimer disease. Arch Neurol 2007;64:1312–7
31. Mufson EJ, Chen EY, Cochran EJ, et al. Entorhinal cortex beta-amyloid load in individuals with mild cognitive impairment. Exp Neurol 1999; 158:469–90
32. Schenk S, Muser J, Vollmer G, et al. Tenascin-C in serum: a questionable tumor marker. Int J Cancer 1995;61:443–9
33. Ikonomovic MD, Abrahamson EE, Isanski BA, et al. X-34 labeling of abnormal protein aggregates during the progression of Alzheimer's disease. Methods Enzymol 2006;412:123–44
34. Arnold SE, Hyman BT, Flory J, et al. The topographical and neuroanatomical distribution of neurofibrillary tangles and neuritic plaques in the cerebral cortex of patients with Alzheimer's disease. Cereb Cortex 1991; 1:103–16
35. Pike KE, Savage G, Villemagne VL, et al. Beta-amyloid imaging and memory in non-demented individuals: evidence for preclinical Alzheimer's disease. Brain 2007;130:2837–44
36. Price JL, McKeel DW, Jr., Buckles VD, et al. Neuropathology of nondemented aging: presumptive evidence for preclinical Alzheimer disease. Neurobiol Aging 2009;30:1026–36
37. Zagzag D, Friedlander DR, Miller DC, et al. Tenascin expression in astrocytomas correlates with angiogenesis. Cancer Res 1995;55:907–14
38. Koukoulis GK, Gould VE, Bhattacharyya A, et al. Tenascin in normal, reactive, hyperplastic, and neoplastic tissues: biologic and pathologic implications. Hum Pathol 1991;22:636–43
39. Eikelenboom P, Veerhuis R, Familian A, et al. Neuroinflammation in plaque and vascular beta-amyloid disorders: clinical and therapeutic implications. Neurodegener Dis 2008;5:190–3
40. Rozemuller AJ, van Gool WA, Eikelenboom P. The neuroinflammatory response in plaques and amyloid angiopathy in Alzheimer's disease: therapeutic implications. Curr Drug Targets CNS Neurol Disord 2005;4: 223–33
41. Zhang WW, Lempessi H, Olsson Y. Amyloid angiopathy of the human brain: immunohistochemical studies using markers for components of extracellular matrix, smooth muscle actin and endothelial cells. Acta Neuropathol 1998;96:558–63
42. Leins A, Riva P, Lindstedt R, et al. Expression of tenascin-C in various human brain tumors and its relevance for survival in patients with astrocytoma. Cancer 2003;98:2430–9
43. Natali PG, Nicotra MR, Bigotti A, et al. Comparative analysis of the expression of the extracellular matrix protein tenascin in normal human fetal, adult and tumor tissues. Int J Cancer 1991;47:811–6
44. Van Eldik LJ, Griffin WS. S100 beta expression in Alzheimer's disease: relation to neuropathology in brain regions. Biochim Biophys Acta 1994; 1223:398–403
45. Sheng JG, Mrak RE, Bales KR, et al. Overexpression of the neuritotrophic cytokine S100beta precedes the appearance of neuritic beta-amyloid plaques in APPV717F mice. J Neurochem 2000;74:295–301
46. Mrak RE, Sheng JG, Griffin WS. Correlation of astrocytic S100 beta expression with dystrophic neurites in amyloid plaques of Alzheimer's disease. J Neuropathol Exp Neurol 1996;55:273–9
47. Sheng JG, Mrak RE, Griffin WS. Neuritic plaque evolution in Alzheimer's disease is accompanied by transition of activated microglia from primed to enlarged to phagocytic forms. Acta Neuropathol 1997;94:1–5
48. Akiyama H, Barger S, Barnum S, et al. Inflammation and Alzheimer's disease. Neurobiol Aging 2000;21:383–421
49. Wyss-Coray T, Rogers J. Inflammation in Alzheimer disease-a brief review of the basic science and clinical literature. Cold Spring Harb Perspect Med 2012;2:a006346
50. Giulian D, Woodward J, Young DG, et al. Interleukin-1 injected into mammalian brain stimulates astrogliosis and neovascularization. J Neurosci 1988;8:2485–90
51. Brellier F, Tucker RP, Chiquet-Ehrismann R. Tenascins and their implications in diseases and tissue mechanics. Scand J Med Sci Sports 2009; 19:511–9
52. Pearson CA, Pearson D, Shibahara S, et al. Tenascin: cDNA cloning and induction by TGF-beta. Embo J 1988;7:2977–82
53. Chiovaro F, Chiquet-Ehrismann R, Chiquet M. Transcriptional regulation of tenascin genes. Cell Adh Migr 2015;9:34–47
54. Midwood K, Sacre S, Piccinini AM, et al. Tenascin-C is an endogenous activator of Toll-like receptor 4 that is essential for maintaining inflammation in arthritic joint disease. Nat Med 2009;15:774–80
55. Nakahara H, Gabazza EC, Fujimoto H, et al. Deficiency of tenascin C attenuates allergen-induced bronchial asthma in the mouse. Eur J Immunol 2006;36:3334–45
56. Mackie EJ, Halfter W, Liverani D. Induction of tenascin in healing wounds. J Cell Biol 1988;107:2757–67
57. Page TH, Charles PJ, Piccinini AM, et al. Raised circulating tenascin-C in rheumatoid arthritis. Arthritis Res Ther 2012;14:R260
58. Martin D, Brown-Luedi M, Chiquet-Ehrismann R. Tenascin-C signaling through induction of 14-3-3 tau. J Cell Biol 2003;160:171–5
59. Di Francesco L, Correani V, Fabrizi C, et al. 14-3-3epsilon marks the amyloid-stimulated microglia long-term activation. Proteomics 2012;12: 124–34
60. Layfield R, Fergusson J, Aitken A, et al. Neurofibrillary tangles of Alzheimer's disease brains contain 14-3-3 proteins. Neurosci Lett 1996;209: 57–60
61. Hashiguchi M, Sobue K, Paudel HK. 14-3-3zeta is an effector of tau protein phosphorylation. J Biol Chem 2000;275:25247–54

62. Agarwal-Mawal A, Qureshi HY, Cafferty PW, et al. 14-3-3 connects glycogen synthase kinase-3 beta to tau within a brain microtubule-associated tau phosphorylation complex. J Biol Chem 2003;278:12722–8
63. Yuan Z, Agarwal-Mawal A, Paudel HK. 14-3-3 binds to and mediates phosphorylation of microtubule-associated tau protein by Ser9-phosphorylated glycogen synthase kinase 3beta in the brain. J Biol Chem 2004;279:26105–14
64. Khachaturian ZS. Diagnosis of Alzheimer's disease. Arch Neurol 1985; 42:1097–105
65. Klunk WE, Engler H, Nordberg A, et al. Imaging brain amyloid in Alzheimer's disease with Pittsburgh Compound-B. Ann Neurol 2004;55: 306–19
66. Curtis C, Gamez JE, Singh U, et al. Phase 3 trial of flutemetamol labeled with radioactive fluorine 18 imaging and neuritic plaque density. JAMA Neurol 2015;72:287–94
67. Clark CM, Pontecorvo MJ, Beach TG, et al. Cerebral PET with florbetapir compared with neuropathology at autopsy for detection of neuritic amyloid-beta plaques: a prospective cohort study. Lancet Neurol 2012; 11:669–78
68. Sabri O, Sabbagh MN, Seibyl J, et al. Florbetaben PET imaging to detect amyloid beta plaques in Alzheimer's disease: Phase 3 study. Alzheimers Dement 2015;11:964–74
69. Ikonomovic MD, Klunk WE, Abrahamson EE, et al. Post-mortem correlates of in vivo PiB-PET amyloid imaging in a typical case of Alzheimer's disease. Brain 2008;131:1630–45
70. Lockhart A, Lamb JR, Osredkar T, et al. PIB is a non-specific imaging marker of amyloid-beta (Abeta) peptide-related cerebral amyloidosis. Brain 2007;130:2607–15
71. Bacskai BJ, Frosch MP, Freeman SH, et al. Molecular imaging with Pittsburgh Compound B confirmed at autopsy: a case report. Arch Neurol 2007;64:431–4
72. Soares HD, Potter WZ, Pickering E, et al. Plasma biomarkers associated with the apolipoprotein E genotype and Alzheimer disease. Arch Neurol 2012;69:1310–7